13th World Conference on Earthquake Engineering
Vancouver, B.C., Canada
August 1-6, 2004
Paper No. 809

EXPERIMENTAL STUDY OF MODEL EMBANKMENT ON LIQUEAFACTION GROUND

Motohiro OHKI[1] Ryo SAWADA[2] Yoshitsugu KANAGUCHI[3] Ayako MIROKU[4]

SUMMARY

Most of the damage of embankment due to liquefaction is mainly caused by the settlement of the whole structure due to the liquefaction of subsoil. The objective of the present study is to evaluate the settlement of embankment based on the degree of liquefaction of subsoil and duration of shaking through a series of experiments with a shaking table. The relationship between the subsidence of embankment and the total deformation including that of subsoil is evaluated quantitatively. The experiment revealed that the settlement of embankment was effectively reduced by the proposed method that can restrain the lateral flow of liquefied subsoil.

INTRODUCTION

A great number of railroad embankments were seriously damaged to accompany large settlements, (as typically shown in Fig. 1), in the 1964 Niigata earthquake. These settlements were mainly caused by the liquefaction of subsoil which was affected by the degree of liquefaction and the continued seismic motion as summarized by Sawada et al, 2003. Even a small settlement of embankment may endanger the safety of train running. Therefor it is necessary to propose a rational and economic method that can reduce the settlement of embankment effectively.

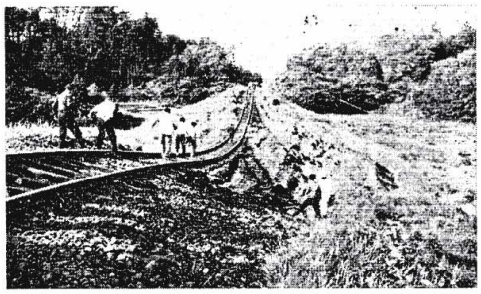

Fig. 1 Damaged embankment of railroad

Based on the test result, a method that can restrain the lateral flow of liquefied subsoil was suggested. The experiment revealed that the settlement of embankment was effectively reduced by the proposed method. In addition, the relationship between the settlement of embankment and the total deformation including that of the subsoil was quantitatively evaluated by a newly developed image processing system using a high-speed CCD camera.

[1] Railway Technical Research Institute, Foundation and Geotechnical Engineering.
[2] Railway Technical Research Institute, Foundation and Geotechnical Engineering.
[3] Railway Technical Research Institute, Foundation and Geotechnical Engineering.
[4] Railway Technical Research Institute, Foundation and Geotechnical Engineering.

TESTING PROCEDURE

Figure 2 shows the Model summary. The model tests were conducted by using a shaking table at the Railway technical Research Institute, Japan. A laminar shear box (2.1m by 1.1m by 1.4m (length by width by height)) was fixed on this table. The deformation of the model can be observed through a transparent wall made of reinforced glass in front of the container.

Figure 2 (1) shows the construction of model, which consists of the subsoil and an embankment with silica sand (D_{50}=0.31mm, Gs=2.652, e_{max}=0.903, e_{min}=0.582). The scale of the embankment model was 1/30, and the height of the actual embankment was about 7.5m. The sand layers were prepared by using a sand hopper. The relative density of the subsoil obtained by this method was 60% and that of the embankment was 80%. In order to increase the degree of saturation of subsoil, CO2 was filled up for the whole subsoil area, and the water was supplied from the bottom of the soil container. In order to avoid the failure of embankment, the water content of embankment was controlled to be at the optimum level by the hydraulic filling method.

Figure 2 (2) shows the arrangement of the typical measurement instruments. As shown in Fig. 2 (2) the vertical lines where accelerometers and piezometers located were named Line-1 and Line-2. In particular, Line-2 is the center of the model. To observe the behavior of deformation and displacement of subsoil and embankment, there were two types of targets. One was made of colored sand, which was adjacent to the transparent wall made of reinforced glass in front of the container. The dynamic displacement of the colored targets was observed by high-speed CCD camera during shaking. Another type was made of plastic with the same unit weight of the sand, which was not only adjacent to the transparent wall, but also extended in the direction of thickness. The displacement of the model can be indicated with coordinates after shaking by the plastic targets.

Figure 2 (3) shows the input acceleration in the experiments. The table was shaken horizontally by using uniformed twenty sinusoidal waves, lasting 6.6sec at the frequency of 3Hz and at amplitude of 300gal.

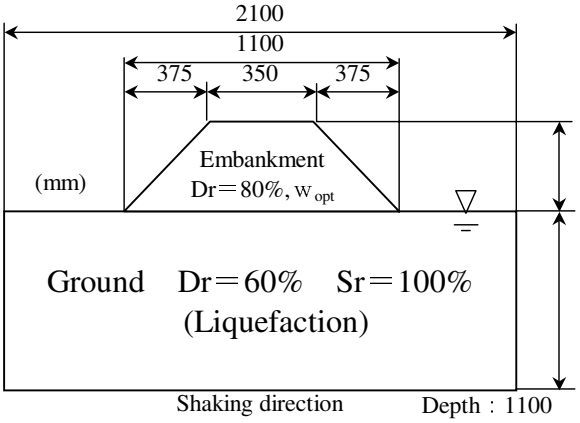

(1) Construction of model

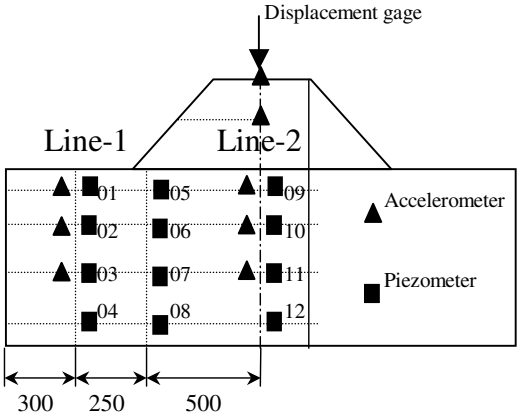

(2) Arrangement of instruments

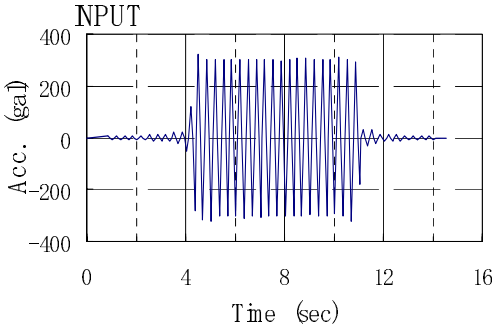

(3) Input acceleration

Fig. 2 Summary of model (Normal type)

TEST RESULTS OF NORMAL MODEL

The failure pattern of the normal model

Figure 3 shows the residual displacement of the normal model observed at the end of shaking. A large vertical settlement of the embankment was observed accompanied with lateral flow of subsoil toward the toe of slope. Although a large lateral deformation was observed with the subsoil, only a vertical displacement was observed at the central line of the subsoil.

Figure 4 shows the position of the targets that were buried in the model indicated with coordinates after shaking. From the Figure on the centerline, it can be seen that the total settlement of embankment is about 97mm and the contribution of the total settlement of the embankment and subsoil is 16% and 84%, respectively.

These observations indicate that the settlement of embankment was mainly caused by the lateral flow and vertical consolidation of the liquefied subsoil. In addition, while the embankment suffered from large deformation, only a small displacement was observed with the plastic targets at the toe of slope.

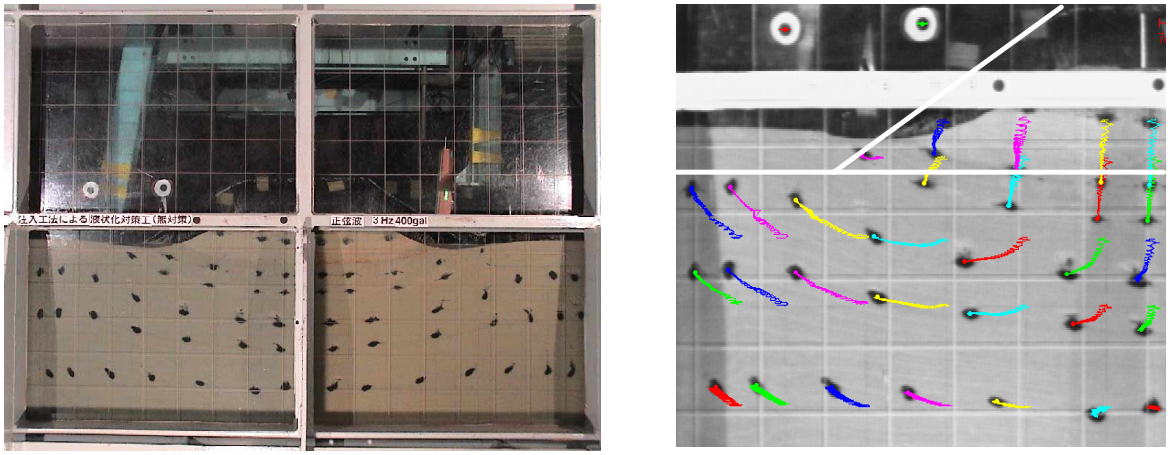

(1) Whole shape (2) Movement of colored sand

Fig. 3 Residual deformation of model

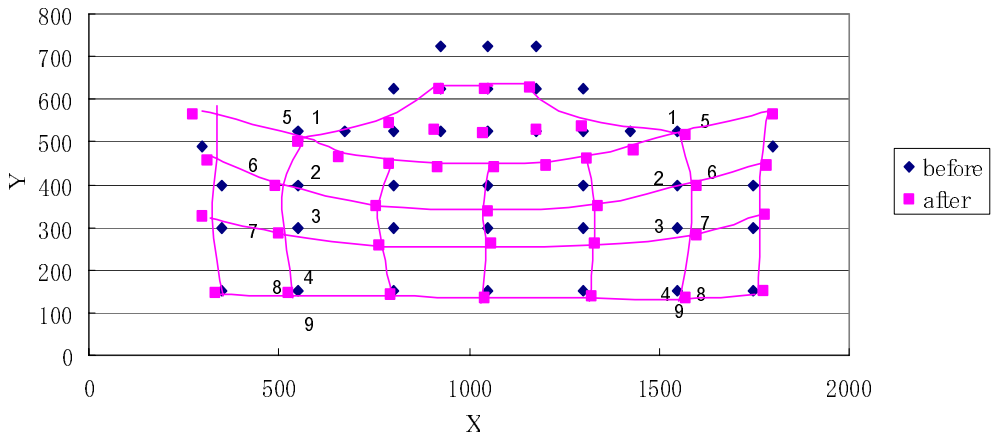

Fig. 4 Position of plastic targets

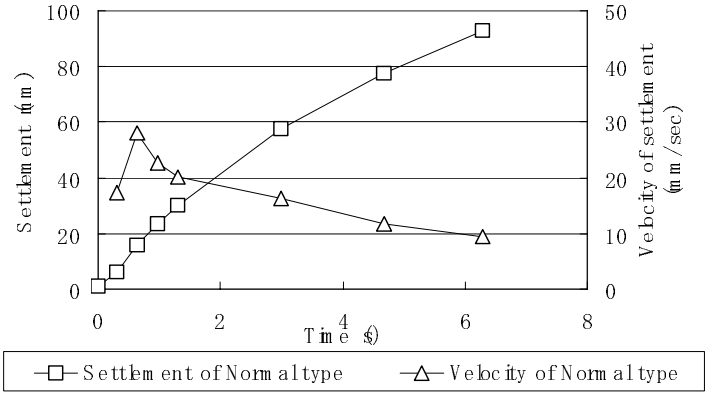

Fig.5 Settlement and the average velocity of settlement (Normal type)

Settlement of embankment

Figure 5 shows the top of the embankment settlement and average settlement velocity (settlement / shaking time) during shaking. Although the average settlement velocity increases at the 3rd peak and decreases thereafter, the whole settlement continues to increase during shaking. The appraising of the settlement takes into account not only the degree of liquefaction but also the duration of seismic motion.

Distribution of acceleration and pore water pressure

Figure 6 shows the relationship between the sinusoidal peak number and the response acceleration measured at Line-1 and Line-2 (Fig. 2 (2)). Line-1 represents the cross section of the free ground; Line-2 over the ground level corresponds to the embankment; and Line-2 under the ground level corresponds to the subsoil under the center of embankment. At Line-1 of the free ground, response acceleration starts decreasing at the 4th peak, and becomes smaller than the base acceleration. At Line-2 of the embankment, it starts decreasing at the 3rd peak and becomes smaller, while that of the subsoil under the central embankment, it also starts decreasing at the 3rd peak, but keeps the response acceleration in the latter half of shaking, remarkable by deep in the subsoil.

Figure 7 shows the relationship between the sinusoidal peak number and the pore water pressure that measured at Line-1 and Line-2. The dotted lines in the Figure shows the relationship between the vertical effective stress and the depth of subsoil. At Line-1, the pore water pressure starts increasing at the 1st peak, and keeps a value similar to that of the effective stress. At Line-2 in the shallow area, it increases gradually, and goes up to a value similar to that of the effective stress. At Line-2 of the subsoil in the deep area, it starts increasing at the 1st peak, but decreases gradually in the latter half of shaking. Therefor, the liquefaction degree at the shallow subsoil increases with the subsoil under the center of the embankment until the end of shaking, but that at the deep part increases in the first half of shaking and decreases in the latter half. It is indicated that the response acceleration at the deep part increases in the latter half. As to the free ground, the liquefaction progresses from the beginning to the end of shaking.

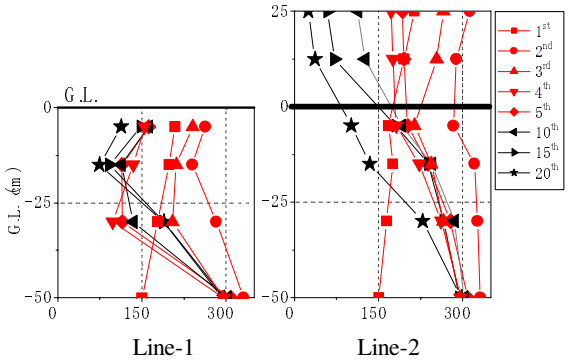

Fig. 6 Relationship between the sinusoidal peak number and the response acceleration

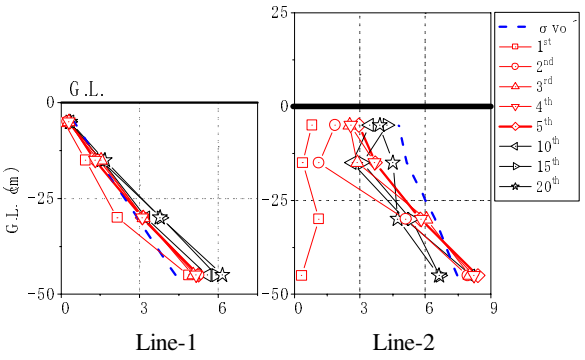

Fig. 7 Relationship between the sinusoidal peak number and the pore water pressure

Contours of excess pore water ratio and displacement of subsoil

Figure 8 shows that the contours of excess pore water pressure ratio and the displacement (the scalar quantity) of subsoil correspond to the each peak number of the sinusoidal waves. Since it is known that the complete liquefaction occurs at the 5th peak from Fig. 5 and Fig. 6, the contours of excess pore water pressure ratio shown in Fig. 7 are normalized at the 5th peak.

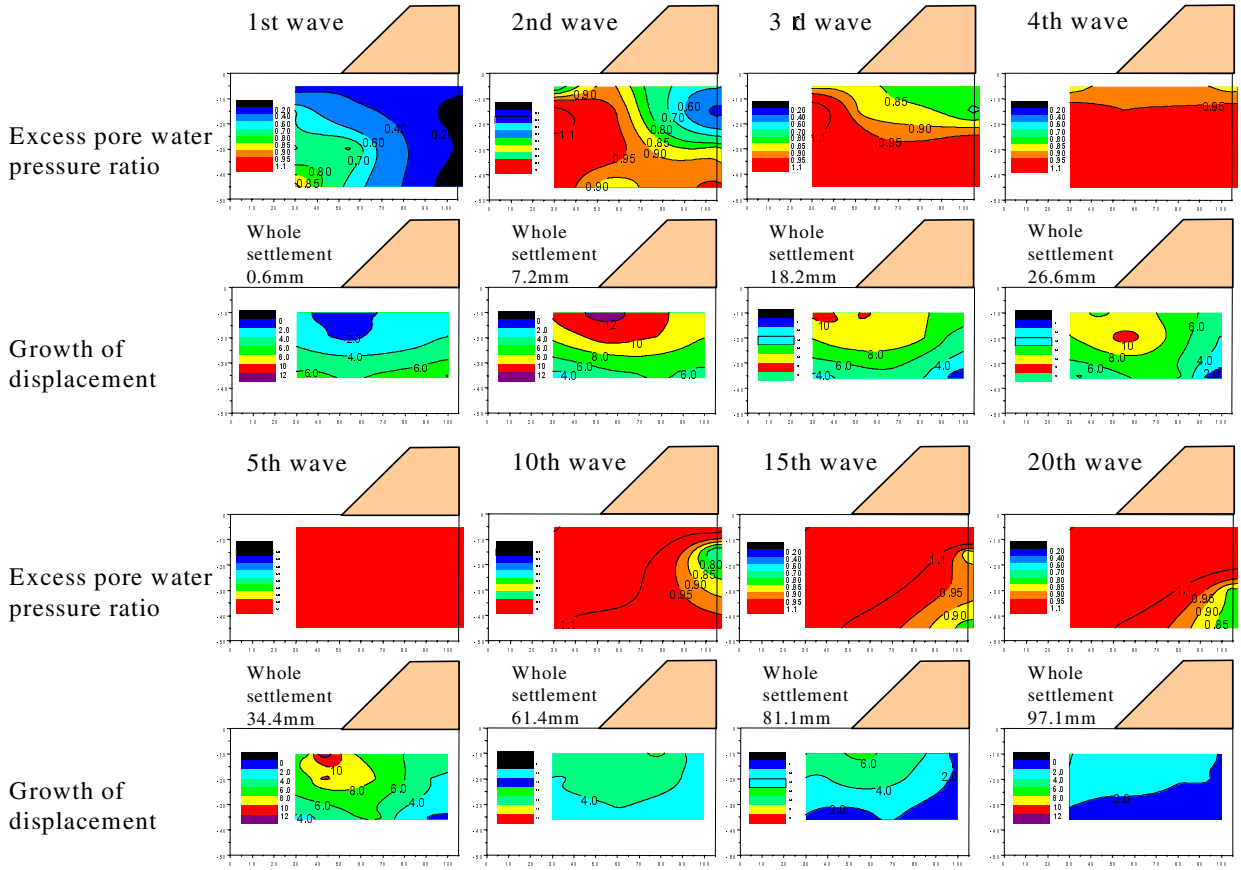

Fig. 8 Contour of excess pore water pressure and the growth of displacement at peak number of waves

The excess pore water pressure ratio rises from the deep subsoil under the toe of slope at the 1st peak. It increases to 1.0 at the 2nd peak, and reaches 1.0 in all the subsoil at the 5th peak. In the latter half of shaking, the excess pore water pressure starts decreasing in the shallow subsoil under the embankment. The lower area of excess pore water pressure ratio in the contour shift to the bottom of subsoil as shaking continues. As the displacement contours of subsoil, it is observed notably that the displacement of subsoil under the toe of slope is larger than that of other parts. In the first half of shaking, the growth of displacement of subsoil under the toe of slope keeps 8 to 10 mm per one wave. In particular, the growth at the 2nd peak is the largest when compared with these at other peaks, or 10 - 12mm per one wave. In the latter half of shaking, the total displacement of subsoil continues increasing slowly until the end of shaking.

TEST RESULT WITH COUNTERMEASURES

From the viewpoint of engineering practice, it is difficult to carry out large-scale countermeasures like the full improvement method under the existing embankment. According to Fig. 7, it is effective to prevent the settlement of the whole embankment by applying a countermeasure at the toe of slope where large displacements occurred due to liquefaction. As to the countermeasures against liquefaction, there are the sand compaction pile method, sand drain method, and so on.

In this paper, it is considered that the part improvement method has advantages such as optional decision of improvement area, economy, and small influence on the existing embankment etc., which is based on the chemical grouting method in the subsoil. Based on the normal model, several types of countermeasure made of gel-improvement bodies were set in the subsoil. The strength and rigidity of the gel-improvement bodies were based on the similarity rule to the actual solidified ground after improvement.

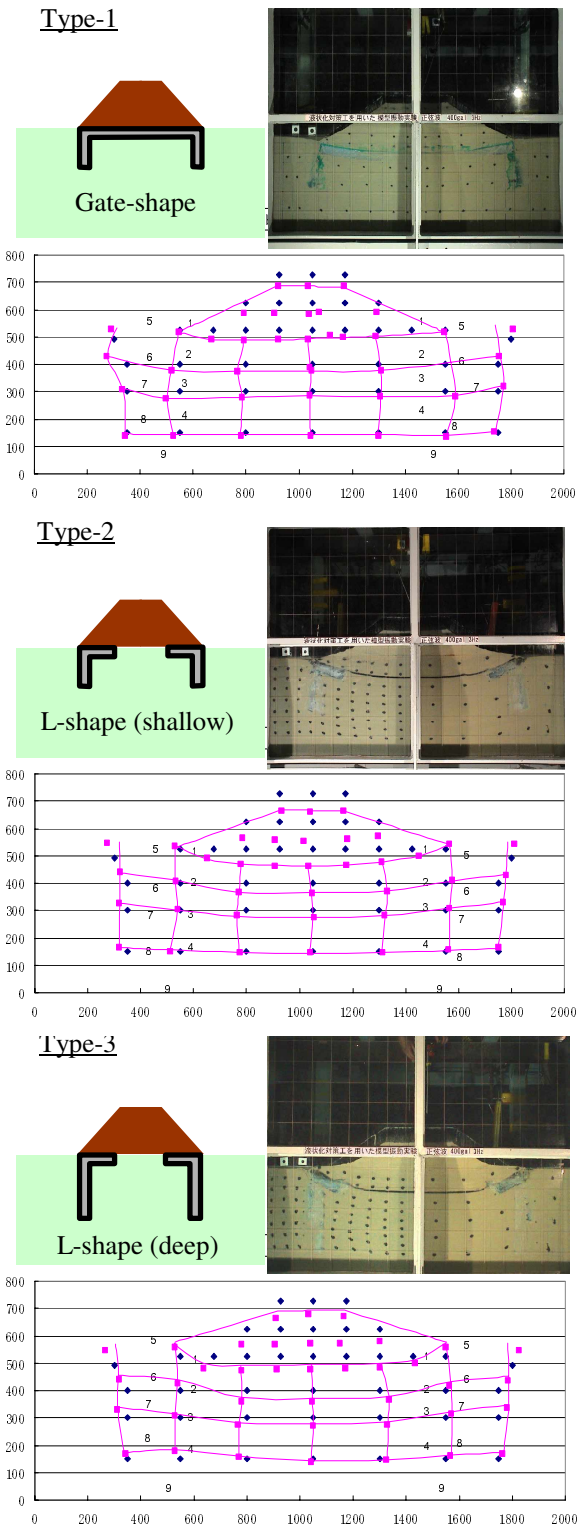

Fig.9 Residual deformation of types
(The whole shape and target)

Summary of the experiments

Table 1 Summary of settlement

Type	Shape	Whole settlement
Normal type	-	97mm
Type-1	Gate shape	48mm
Type-2	L-shape (shallow)	75mm
Type-3	L-shape (deep)	70mm

Figure 9 shows the residual displacement of the models with countermeasures observed at the end of shaking, and the position of the plastic targets that are buried in the model indicated with coordinates after shaking. The whole settlement and that of embankment itself corresponding to each countermeasure and the normal type are shown in Table 1. The settlements of the embankment with countermeasures are smaller than that of the normal type. The countermeasure for Type-1 is more effective than that for Type-2 and Type-3. In Type-2 and Type-3, there is little relative movement of gel-improvement body. Only the revolving improvement body around the toe of slope on the spot is observed.

Response acceleration and settlement of embankment

Figure 10 shows the relationship between the shaking time and response acceleration, settlement and settlement velocity of the top of embankment. The response accelerations with countermeasures are not dependent on the type of countermeasure, and are larger than that of normal type. It is observed that the response acceleration of embankment increases caused by the improvement of subsoil. The settlement of Type-3 is almost the same as that of Type-1 at the beginning of shaking, and the same as that of Type-2 at the end of shaking. It is also observed that the settlement velocity of Type-3 is equal to that of Type-1 before the peak. When comparing with other cases, the settlement velocity of Type-3 decreases gently after the peak, so the whole settlement is larger than in other cases in the latter half of shaking. The peak time of the Type–3 is at the 3rd peak, while those in other cases are at the 2nd peak.

The distribution of excess pore water pressure ratio

Figure 11 shows the behavior of the excess pore water pressure ratio corresponding to each countermeasure. The 5th and 20th waves are shown as contours in this Figure. The relationship between excess pore water pressure ratio and time corresponding to the three

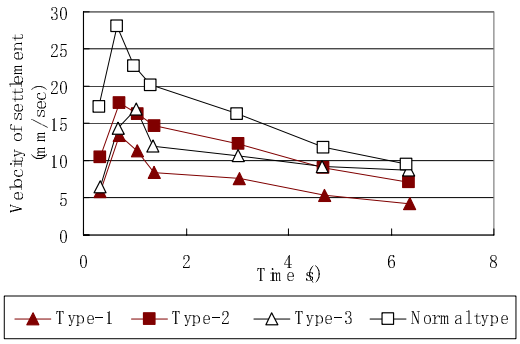

(1) Response acceleration of the top of embankment

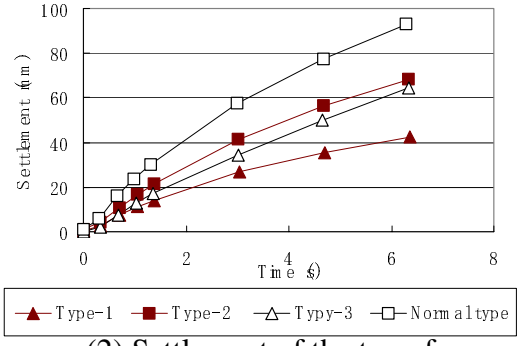

(2) Settlement of the top of embankment

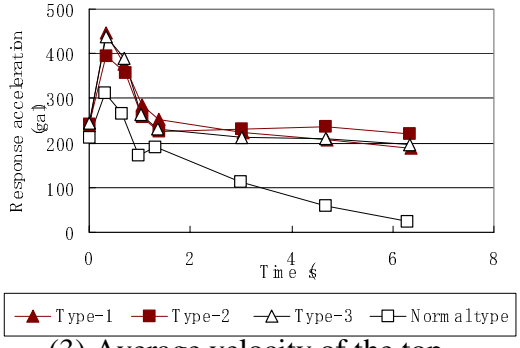

(3) Average velocity of the top of settlement

Fig.10 Relationship between the response value and shaking time

different depths are also shown. In regard to the circumstances of counter-measure, the arrangement of the instruments was changed for the normal type. As an example, Fig. 12 shows the case of Type-1. The arrangements of Type-2 and Type-3 are the same as that of Type-1.

The distribution of excess pore water pressure ratio depends on the type of countermeasure. As to Type-1, the excess pore water pressure ratio of the free ground is very low when compared with that in other cases. Because of the low degree of liquefaction in the free ground, there is little lateral flow of the subsoil under the embankment. As to Type-2 and Type-3, the excess pore water pressure ratio of the subsoil under the embankment is smaller than that of the normal type. The distributions of excess pore water pressure ratio in the two cases are similar, whose pattern depends on the shape of countermeasure. In particular, the excess pore water pressure ratio at 06 (in Fig. 11) of Type-3 maintains a high value continuous during shaking. Therefore, the settlement velocity decreases more gently than other cases in latter half of shaking. It is known that the distribution of excess pore water pressure ratio is changed by the types of countermeasures.

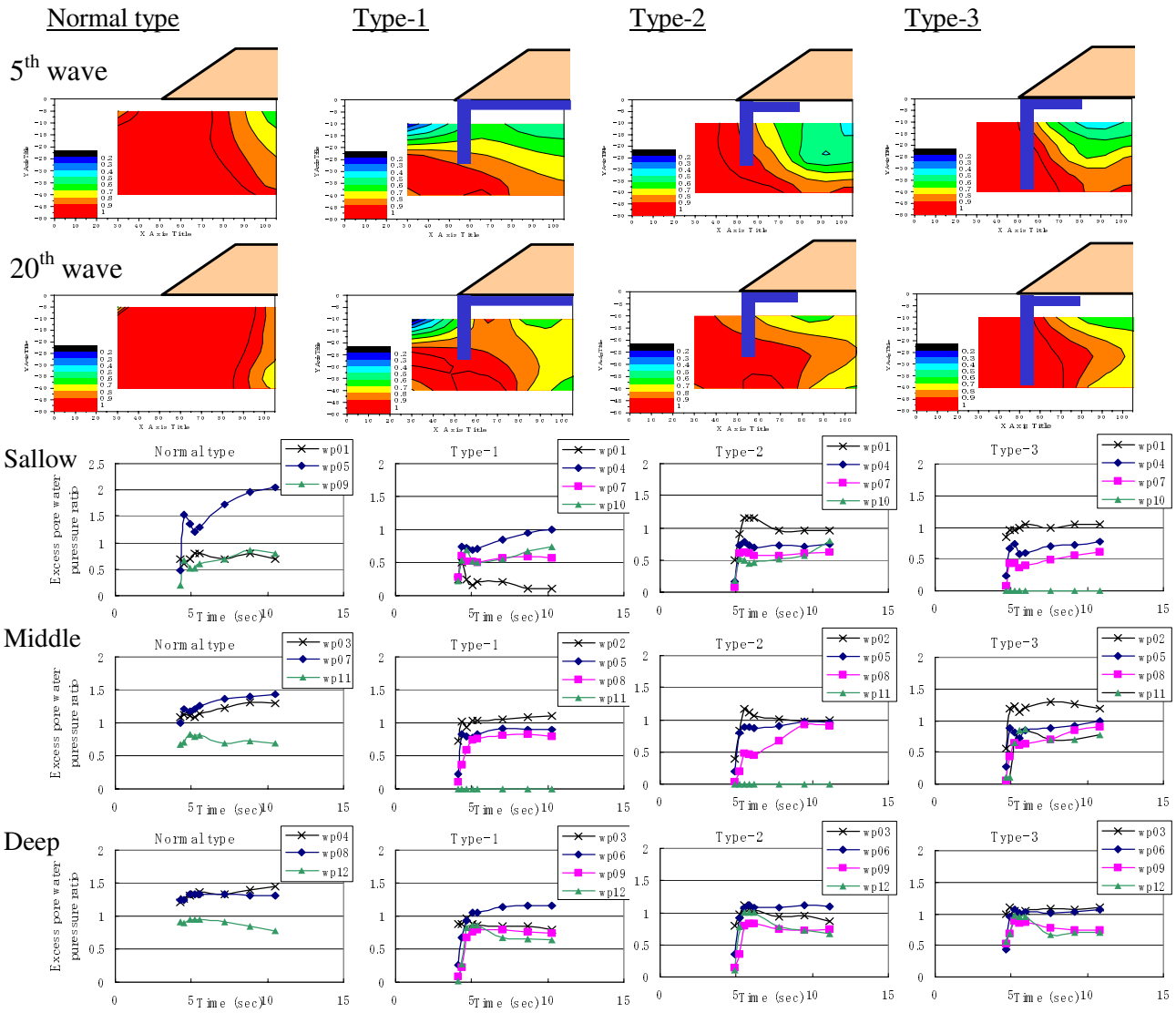

Fig.11 Relationship between shaking time and excessive pore water ratio in subsoil

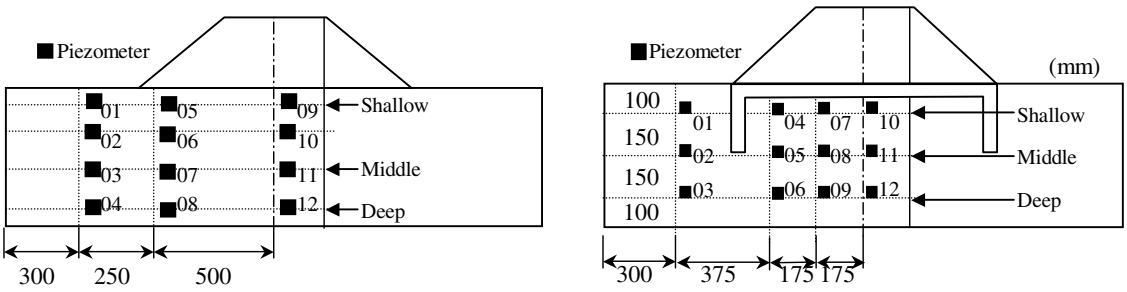

(1) Arrangement in Normal type (2) Arrangement in Type-1

Fig.12 Arrangement of instrument

DISCUSSION OF RESULTS

According to Fig. 4 and Fig. 9, the position of the target at the toe of slope moved slightly after shaking. Thus, the toe of slope can be considered as a fixed point. Sasaki et al. (1992) carried out shaking table tests to draw a conclusion, as the volume of sand is kept constant during the period when a lateral flow is observed. Towhata et al. (1999) explained that this point means that the consolidation settlement after liquefaction should be considered separately. Therefor, the factors of the whole embankment settlement should be concerned with the lateral flow, consolidation settlement of subsoil and the settlement of the embankment itself. Given in Fig. 13 is a conceptual explanation of the settlement due to the above primary factors.

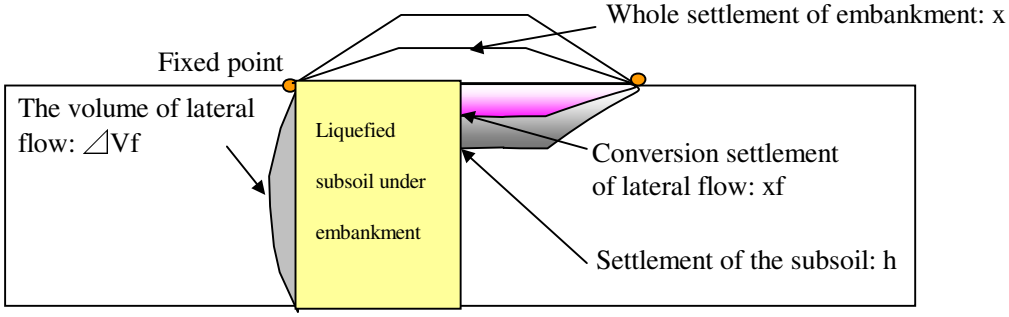

Fig. 13 Primary factors of settlement

Here
x : Whole settlement of embankment
h : Settlement of subsoil under the embankment
xf : Conversion settlement of lateral flow of subsoil
xp : Consolidation settlement of subsoil
xs : Settlement of embankment itself

If the volume of sand is kept constant during the lateral flow of subsoil, that volume is almost the same as the product of the settlement and the width of the embankment. Thus, the volume of lateral flow of subsoil (ΔVf) can convert into the settlement of embankment. Although the bottom of the embankment after shaking is formed circular, the shape is approximately by the same as that is shown in Fig. 14.

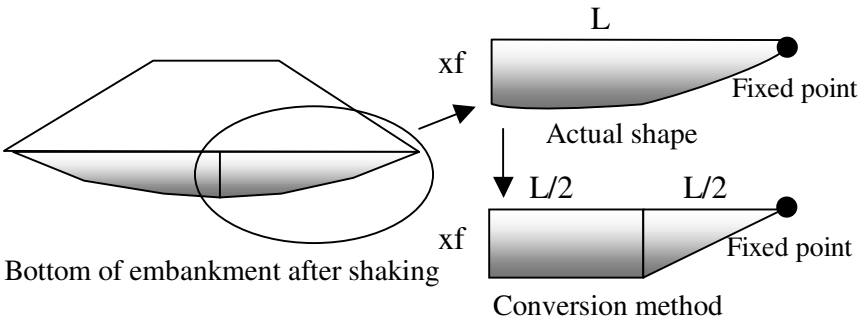

Fig. 14 Conversion method from lateral flow to settlement

In this case, the embankment bottom is approximating square at the center side and the triangle at the other side. Therefore, the following three types of settlement can be derived.

$\triangle Vf = (L/2)^* x f + ((L/2)^* x f)/2 = 0.75L^* x f$

$x f = \triangle Vf / 0.75L$

$x p = h - x f$

$x s = x - h = x - x f - x p$

Figure 15 shows the evaluation result of the above types of settlement. Each part of settlement in Type-1 decreases corresponding to that of the normal type. In particular, the consolidation settlement of subsoil decreases 64%. Consolidation occurs to draining of pore water, but it is impossible to drain from the free ground because the pore water pressure does not rise enough to become liquefied in this case. Therefore, little consolidation settlement occurs due to the pore water in subsoil. According to the result of Type-2 and Type-3, the effect of preventing the lateral flow by the countermeasure is confirmed, but the consolidation settlement is raised. A reason for this phenomenon is that the countermeasure of gel-improvement body moved to a different phase from the subsoil with the increase in the excess pore water pressure during shaking, which was observed with a high-speed CCD camera. Therefore, the improvement body removed to the subsoil periodically. The pressured pore water flows around the improvement body as a water path. Then, the consolidation settlement occurs. It is known that the factors of settlement of embankment are different according to the types of countermeasures.

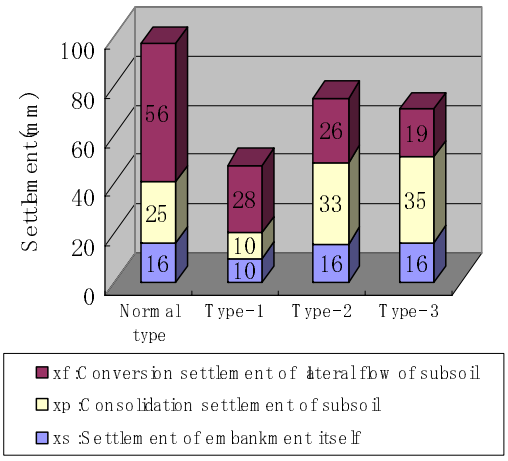

Fig.15 the ratio of primary factors to whole settlement

CONCLUSIONS

1. According to the experimental result of the normal type, the displacement of the subsoil is remarkable under the toe of slope, but the toe of slope moves slightly during shaking.
2. The subsoil under the center of embankment settles vertically.
3. As the pore water pressure of subsoil rises, the response acceleration of the embankment decreases.
4. The evaluation of settlement should take into account not only the degree of liquefaction but also the duration of shaking.

5. According to the result in experiments with countermeasures, it is possible to make the whole settlement decrease by applying the countermeasure at the toe of slope.
6. The factors of the whole embankment settlement are the lateral flow of subsoil, settlement of the embankment itself and consolidation settlement of subsoil.
7. The distribution of excessive pore water pressure ratio and the factors of whole settlement are different depending on the type of countermeasure.

REFERENCES

1. Nasu, M., (1995). "Relationship between Structures of Sandy Ground and Liquefaction-Induced Damage to Various Objects" Quarterly Report of RTRI, Vol. 36, No. 2, Jun. '95. (in Japanese)
2. Sawada, R., Miroku, A., Ohki, M. Kanaguchi, Y. Teshigawara, A., and Tateyama, M. (2003). "Experimental studies of model embankments on liquefaction ground (Part 1,2)" Proceeding. Japan National Conference Geotechnical Engineering, Vol.2, pp.1315-1318. (in Japanese)
3. Sasaki, Y., Towhata, I., Tokida, K., Yamada, K., Matsumoto, H., Tamari, Y. and Saya, A. (1992):"Mechanism of permanent displacement of ground caused by seismic liquefaction" Soils and Foundations, Vol.32, No.3, pp.73-90.
4. Towhata, I., Orense, R. P. and Toyota, H. (1999):"Mathematical principles in prediction of lateral ground displacement induced by seismic liquefaction" Soils and Foundations, Vol.39, No.2, pp.1-19.
5. Kanaguchi, Y., Sawada, R., Miroku, A. and Ohki, M. (2003)."Experimental studies of model embankments on liquefaction" JSCE Journal of Earthquake Engineering, Vol.27, Paper No.93.